Self-cleaning Properties of TiO_2/palygorskite and TiO_2/halloysite Nanocomposite Coatings

Dionisios Panagiotaras[a], Eleni Kaplani[a], Elias Stathatos[b,*], Dimitrios Papoulis[c]

[a]*Mechanical Engineering Department, Technological-Educational Institute of Western Greece, 26334 Patras, Greece*
[b]*Electrical Engineering Department, Technological-Educational Institute of Western Greece, 26334 Patras, Greece*
[c]*Geology Department, University of Patras, 26504 Patras, Greece*
[*]*correspondence should be addressed: email address: estathatos@teipat.gr*

Abstract. Tubular halloysite and microfibrous palygorskite clay mineral combined with nanocrystalline TiO_2 are involved in the preparation of nanocomposite films on glass substrates via sol-gel route at 450ºC. The synthesis employing nonionic surfactant molecule as pore directing agent along with the acetic acid-based sol-gel route without addition of water molecules. Drying and thermal treatment of composite films ensure elimination of organic material lead to the formation of TiO_2 nanoparticles homogeneously distributed on the palygorskite and halloysite surfaces. Nanocomposite films without cracks of active anatase crystal phase on palygorskite and halloysite surfaces are characterized by microscopy techniques, UV-Vis spectroscopy, and porosimetry methods in order to examine their structural properties. The composite palygorskite-TiO_2 and halloysite/TiO_2 films with variable quantities of palygorskite and halloysite were tested as photocatalysts in the photo-oxidation of Basic Blue 41 azo dye in water. These nanocomposite films proved to be most promising photocatalysts and highly effective to dye's decoloration in spite of small amount of palygorskite/TiO_2 or halloysite/TiO_2 catalyst immobilized onto glass substrates.

Keywords: Titanium dioxide; nanocrystalline; clay mineral; Palygorskite; Halloysite; Photocatalysis; Sol-gel method.
PACS: 81.07.-b; 81.07.Bc; 81.16.-c; 81.16.Be; 81.16.Hc; 81.16.Pr.

INTRODUCTION

Nowadays water pollution has become one of the most serious problems worldwide. A variety of organic and inorganic pollutants produced by anthropogenic activities affect water quality and in some cases render water a rare element for consumption by humans. Degradation of various organic pollutants by photocatalysis, using wide band gap semiconductors under UV or solar light, has been extensively studied [1-3]. In the case of organic pollutants, azo dyes are being used in huge quantities for example in the textile industry. The presence of dye in the wastewater of the textile industry affects the photosynthetic process and generates toxicity to the aquatic organisms and also humans [4-6]. The use of highly porous materials such as clay minerals can be considered as alternative substrates for TiO_2 immobilized particles [7-8]. Halloysite clay mineral with tubular structure could be considered as suitable and also cheap material for TiO_2 particles immobilization [9-10]. In addition palygorskite clay mineral microfibers combined with TiO_2 have been used for the decomposition of NOx gases and toluene [11-12].

In this work we present the fabrication of thin mesoporous nanocrystalline TiO_2 composite films with halloysite and palygorskite clay minerals. The enhanced photocatalytic activity of TiO_2 nanoparticles in combination with halloysite nano tubes and palygorskite microfibers was examined to the discoloration of azo-dye Basic Blue 41 in aqueous solutions.

MATERIALS SYNTHESIS AND CHARACTERIZATION

Commercially available Triton X-100 (X100, polyethylene glycol tert-octylphenyl ether), titanium tetraisopropoxide (TTIP), acetic acid (AcOH), Basic Blue 41 (BB-41) and all solvents were purchased from Sigma-Aldrich. Double distilled water with resistivity 18.2 MΩ (Millipore) was used in all experiments. Palygorskite-rich samples (PAL) from Ventzia continental basin, Western Macedonia Greece. Pure and well crystalline halloysite samples (HAL) with tubular morphology were originated from Utah, USA. A amount of X100 was homogeneously dissolved in ethanol (EtOH). Titania precursor, TTIP was added at a time under vigorous stirring. The molar ratio of the materials was optimized at X100:EtOH:AcOH:TTIP=1:69:6:1 in accordance to previous results [13-14].

International Conference of Computational Methods in Sciences and Engineering 2014 (ICCMSE 2014)
AIP Conf. Proc. 1618, 362-365 (2014); doi: 10.1063/1.4897748

Palygorskite powder was mixed with previous solution in various quantities following PAL weight ratio 0%, 33%, 50%, 65%, 75% compared to TiO_2. Films prepared on glass slides for the five PAL-TiO_2 weight ratios will be referred as PAL0, PAL33, PAL50, PAL65 and PAL75 respectively. In addition, halloysite powder was mixed with previous solution in various quantities following HAL 5%, 20%, 25% and 30% weight ratio compared to TiO_2. Samples, abbreviated as HAL5, HAL20, HAL25 and HAL30, while HAL0 is referred to pure TiO_2 films. After several minutes, the dispersion was ready to be used on glass slides. Films prepared on glass slides for the four HAL weight ratios will be referred as HAL5, HAL20, HAL25 and HAL30 respectively while HAL0 represents pure TiO_2 films without the presence of halloysite.

A Bruker D8 Advance diffractometer with CuKα (λ = 1.5406 Å) radiation and Bragg-Brentano geometry was employed for X-ray diffraction (XRD) studies of the PAL-TiO_2 and HAL-TiO_2 catalyst. The XRD patterns showed the halloysite, palygorskite and TiO_2 anatase peaks. Nitrogen intrusion/extrusion curves were measured with a Micromeritics Tristar 3000 and the surface area, porosity, and pore size distribution were derived by differentiating them according to BET method for the HAL-TiO_2 (Table 1).

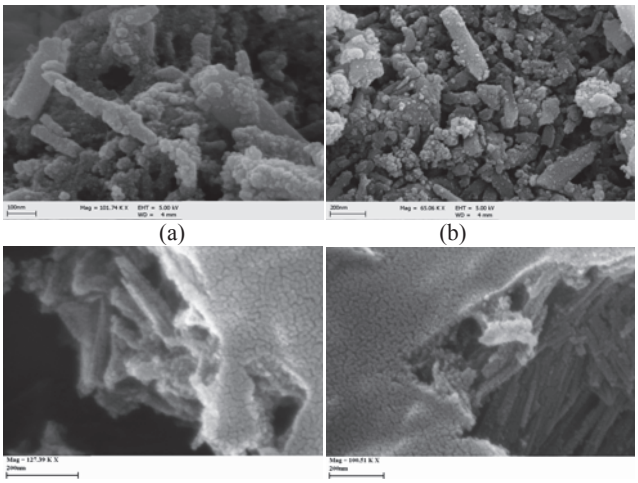

FIGURE 1. SEM images of: (a) HAL5 (b) HAL25 and (c) PAL65 low magnification, (d) PAL65 high magnification films.

TABLE 1. Structural characteristics of PAL-TiO_2 and HAL-TiO_2 films

Sample	Total pore volume Vp (cm^3/g)	Mean pore diameter D_{por} (nm)	Total porosity φ(%)	Specific surface area S (m^2/g)
Palygorskite	3.14	18.0	85.80	123.1
PAL33	0.77	30.1	63.50	65.9
PAL50	0.92	36.0	66.20	82.2
PAL65	1.00	26.5	67.50	100.0
PAL75	1.21	24.7	70.50	95.1
Halloysite	0.125	9.85	24.46	50.9
TiO_2	0.133	4.78	33.58	121.3
HAL5	0.165	6.09	39.10	108.6
HAL20	0.155	7.98	37.62	77.5
HAL25	0.171	7.20	39.95	95.3
HAL30	0.159	6.01	38.21	106.2

However, Hg porosimetry measurements were performed for PAL-TiO_2, instead of BET measurements that are, usually, used for the characterization of titania films. Hg porosimetry measurements are performed in order to obtain

information for pore sizes larger than 0.5 μm, which are not attainable by gas sorption. For porosity measurements, the mercury intrusion curves of all samples were taken with a Quantachrome PoreMaster 60 Mercury Porosimeter while the surface area, porosity, and pore size distribution were derived by curves' differentiation (Table 1). For the visual morphology of PAL-TiO_2 and HAL-TiO_2 nanostructure, an environmental scanning electron microscope (FESEM, Zeiss SUPRA 35VP) was used and inspect film homogeneity [Fig. 1 (a)-(d)]. Absorption measurements of BB-41 sols were carried out with a Hitachi U-2900 UV-Vis spectrophotometer.

In both HAL-TiO_2 and PAL-TiO_2 nanocomposites decomposition kinetics of BB-41 has been observed to follow first-order kinetics and it is well established that photo-discoloration experiments follow Langmuir-Hinshelwood model, where the reaction rate, r, is proportional to the surface coverage, θ, according to the following equation 1 [15]:

$$r = -\frac{dC}{dt} = k_1 \vartheta = \frac{k_1 K C}{1 + KC} \tag{1}$$

where k_1 is the reaction rate constant, K is the adsorption coefficient of the reactant and C is the reactant concentration. In the case that C is very small, KC factor is negligible in respect to unity and the above equation describes first-order kinetics. The integration of the above equation yields to the following equation 2:

$$-\ln\left(\frac{C}{C_0}\right) = k_{app} t \tag{2}$$

With limit condition that on t=0 we have the initial concentration C_0. k_{app} is the apparent first-order rate constant.

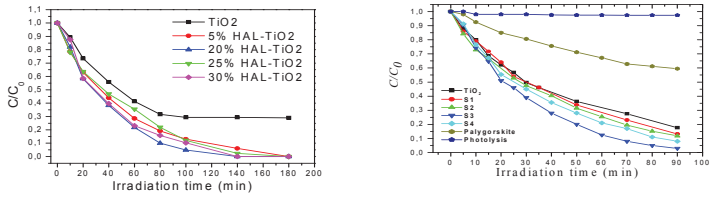

(a) (b)

FIGURE 2. (a) Photo-discoloration of BB-41 by TiO_2 films in presence of different weight percentages of halloysite under UV light. (b) Photodecoloration of BB-41 by different PAL-TiO_2 catalysts. S1, S2, S3 and S4 refer to PAL33, PAL50, PAL65 and PAL75 respectively.

In the case of HAL20 a complete decolorization was reached within 140 min of illumination implied the synergistic effect between clay mineral and TiO_2 by preparing highly porous HAL-TiO_2 catalysts [Fig. 2(a)]. In the case of PAL65 a complete discolorization was reached within 90 min of illumination implied the synergistic effect between palygorskite and TiO_2 by preparing highly porous PAL-TiO_2 catalysts. However, the further addition of palygorskite in films (PAL75) caused a slight decrease on the photocatalytic activity of films [Fig. 2(b)].

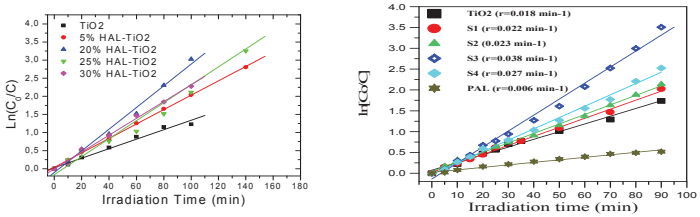

(a) (b)

FIGURE 3. Ln(C_0/C) as a function of irradiation time for: (a) HAL-TiO_2 and (b) PAL-TiO_2 photocatalysts. S1, S2, S3 and S4 refer to PAL33, PAL50, PAL65 and PAL75 respectively.

Discoloration kinetics of BB-41 in presence of different HAL proportions in TiO_2 nanocrystalline films is presented in Fig. 3(a). The maximum value for rate constant was calculated for sample HAL20 (29.8×10^{-3} min^{-1}) while the value for pure TiO_2 film was estimated at 12.9×10^{-3} min^{-1}. Furthermore, all the samples HAL-TiO_2 exhibited better performance than pure TiO_2. We mainly attribute this behavior to the internal light scattering because of the presence of the halloysite. In addition discoloration kinetics of BB-41 in presence of different PAL/TiO_2 proportions is presented in Fig. 3(b). The maximum value for rate constant was calculated for sample PAL65 (38×10^{-3} min^{-1}) while the value for pure TiO_2 film was estimated at 18×10^{-3} min^{-1}. Furthermore, all the

samples PAL/TiO_2 exhibited better performance than pure TiO_2. This is attributed to better structural characteristics of the films compared to pure titania film tabulated at porosity and particle surface area.

The above findings for the HAL-TiO_2 and PAL-TiO_2 nanocomposites could be also attributed to better structural characteristics of the films compared to pure TiO_2 film mainly tabulated at porosity and total pore volume. However, the rate of dye discolorization depends on adsorption of the dye into the catalyst porous structure. Finally, it has been found that the same photocatalysts can be used in several photocatalytic cycles without remarkable loss to their efficiency.

CONCLUSIONS

Both the HAL-TiO_2 and PAL-TiO_2 films exhibited enhanced structural properties including crystallinity and active anatase phase, while enhanced photocatalytic properties to the discoloration of BB-41 in water were succeeded. The experiments on photocatalytic discoloration of BB-41 indicated the importance of preparing highly porous HAL- TiO_2 and PAL-TiO_2 films where a synergistic effect between halloysite tubes and palygorskite microfibers with the TiO_2 nanoparticles could be occurred.

ACKNOWLEDGMENTS

The authors would like to acknowledge financial support from the European Union (Lead Market European Research Area Network - LEAD ERA) and the Regional Authority of Western Greece under the project "INDOOR ECOPAVING". The project is implemented under the Operational Program "DEPIN 2007-2013" Priority Axis (PA) 'Digital convergence and entrepreneurship in Western Greece', action "Transnational Business Collaboration Western Greece" and is co-funded by the European Union –European Regional Development Fund and National Resources (NSRF 2007-2013). Besides, the authors are thankful to Dr. V. Dracopoulos, FORTH/ICE-HT, for his help to the FE-SEM images.

REFERENCES

1. M. N. Chong, B. Jin, C.W.K. Chow and C. Saint, *Water Res.*, **44,** 2997-3027 (2010).
2. H. Choi, S. Al-Abed, D.D. Dionysiou, E.Stathatos and P.Lianos, "TiO_2-Based Advanced Oxidation Nanotechnologies for water Purification and Reuse," in *Sustainability Science and engineering: Sustainable Water Recycling Versus Desalination Contribution,* Sustainability Science and Engineering, **2,** Elsevier, 229-254 (2010).
3. Ahmed, M. G. Rasul, W. N. Martens, R. Brown and M. A. Hashib, *Desalin.*, **261,** 3-18 (2010).
4. G. A. Umbuzeiro, H.S. Freeman, S. H. Warren, D. P. Oliveira, Y. Terao, T. Watanabe and D. D. Claxton, *Chemosp.*, **60,** 55-64 (2005).
5. Y.E. Benkli, M.F. Can, M. Turan and M.S. Çelik, *Water Res.,* **39,** 487-493 (2005).
6. E. Forgacs, T. Cserháti and G. Oros, *Environ. Int.,* **30,** 953-971 (2004).
7. L. Bouna, B. Rhouta, M. Amjoud, F. Maury, M.-C. Lafont, A. Jada, F. Senocq and L. Daoudi, *Appl. Clay Sci.*, **52,** 301-311 (2011).
8. T. An, J. Chen, G. Li, X. Ding, G. Sheng, J. Fu, B. Mai and K. E. O'Shea, *Catal. Today*, **139,** 69-76 (2008).
9. D. Papoulis, S. Komarneni, A. Nikolopoulou, P. Tsolis-Katagas, D. Panagiotaras, H.G. Kacandes, P. Zhang, S. Yin, T. Sato and H. Katsuki, *Appl. Clay Sci.,* **50,** 118-124 (2010).
10. D. Papoulis, S. Komarneni, D. Panagiotaras, E. Stathatos, K. C. Christoforidis, M. Fernández-García, H. Li, Y. Shu, T. Sato and H. Katsuki, *Appl. Catal. B: Environ.*, **147,** 526-533 (2014).
11. D. Papoulis, S. Komarneni, D. Panagiotaras, A. Nikolopoulou, H. Li, S. Yind, Sato Tsugio and H. Katsuki, *Appl. Clay Sci.,* **83-84**, 191-197 (2013).
12. D. Papoulis, S. Komarneni, D. Panagiotaras, A. Nikolopoulou, K.C. Christoforidis[d], M. Fernández-Garcia, H. Li, Y. Shu and T. Sato, *Appl. Clay Sci.,* **83-84,** 198-202 (2013).
13. E. Stathatos, P. Lianos and C. Tsakiroglou, *Micropor. and Mesopor. Mat.*, **75,** 255-260 (2004).
14. H. Choi, E. Stathatos and D. D. Dionysiou, *T. Sol. Films*, **510,** 107-114 (2006).
15. A.O. Ibhadon, G.M. Greenway, Y. Yue, P. Falaras and D. Tsoukleris, *Appl. Catal. B: Environ.,* **84,** 351-355 (2008).